Wave Energy Output Power Design Based on Machine Learning

Wave Energy Output Power Design Based on Machine Learning

Yi Shen, Yihang Wu and Weimei Zhi*

School of Computer and Artificial Intelligence, Zhengzhou University, Zhengzhou 450001, China

Email address of the first author: yshen9_9@outlook.com

Abstract. In recent years, with the excessive use of non-renewable energy sources, energy shortage has become a major problem for countries around the world, and the development of marine renewable energy has become urgent. As an important renewable energy source in the future, wave energy is one of our important research objects. This paper completes the design of the maximum wave energy output power and establishes the motion model of the float and the oscillator and the optimization model of the maximum average output power in the wave energy devices. This work helps people use wave energy reasonably and provides theoretical support for designing a new generation of wave energy equipment. In this paper, the motions of the float and oscillator in this wave energy device are modeled by Newton's theorem and Lagrange's equation, and then the displacement and velocity of the float and oscillator under the pendulum motion at different moments are solved by using the fourth-order Runge-Kutta method. The maximum average output power of the PTO system is solved by building an optimization model with a constant damping coefficient and a non-damping coefficient, followed by the traversal method and genetic algorithm.

1. Introduction

In recent years, influenced by environmental degradation and economic crisis, more people hope to vigorously develop renewable energy [1]. Scientists have found that wave energy has an extremely high energy density [2], with wave power generation attracting widespread attention as its main form of development. Wave power devices can work in a variety of complex environments, which is expensive and difficult to study through offshore experiments alone [3]. Combining mathematical modeling and analysis, it is cheaper and easier to achieve.

To improve the efficiency of the wave energy generation system and maximize the output power, the motion of the float and vibrator in the wave energy device is simulated by Newton's law and Lagrange equation. The fourth-order Runge-Kutta method is used to solve the average output power of the PTO system by using the damping vibration equation of multiple degrees of freedom. The float and oscillator are balanced in static water at the initial moment. When the damping coefficient is fixed and the damping coefficient is changed, the excitation forces of the float and oscillator in the wave are calculated respectively. The displacement and velocity of the float and oscillator at different times are given [4]. In this paper, by integrating the displacement and velocity of vertical oscillation with the angular displacement and velocity of longitudinal oscillation, the output power equation of the float is derived, and an optimization model is established to solve the maximum output power and the corresponding optimal damping coefficient under different damping coefficients, so as to maximize the average output

power of the PTO system. It provides a feasible method to improve the output power of the wave power generation system.

The main innovations and contributions of this paper are as follows:

- This paper focuses on the importance of wave energy in the utilization of renewable energy and uses mathematical modeling to establish and optimize the wave energy output power model to reduce the cost of field investigation.
- In this paper, wave energy output models are established under the two conditions that the damping coefficient of the linear damper takes a value within [0, 100000] and the damping coefficient is proportional to the absolute value of the relative velocity of the float and the oscillator within [0, 100000], extending the application range of the model.
- In this paper, with the help of MATLAB software, the traversal method and genetic algorithm are used to solve and draw the established model, and the relationship between the maximum output power and the optimal damping coefficient is visually expressed.
- This paper compares the time consumed by the traversal method and the genetic algorithm to solve the model and draws the conclusion that the genetic algorithm has the advantage in time complexity when solving such problems.

2. Model Assumptions and Notation

2.1. Assumptions

We make the following assumptions about the model to highlight the core factors of the problem and reduce the impact of secondary factors:

- Seawater is an ideal fluid, non-viscous, non-rotating and non-compressible.
- In damped motion, the spring static deformation and the effect of gravity cancel each other out.
- The system under the action of linear periodic micro-amplitude waves from the initial moment downward motion, the following is positive, the initial moment is the origin of coordinates and potential energy is zero.
- The center of gravity G of the float is on the waterline surface [5].
- The PTO is within the working range and does not exceed the elastic limit of the spring.

2.2. Notations

Important notations used in this paper are listed in Table 1.

Table 1. Symbol description and noun definition.

Symbol	Definition	Symbol	Definition
Z	The displacement of the float by the pendulum motion	M_h	Additional mass under wave action
F_e	Wave excitation force in the direction of pendulum movement on the float	x	The motion displacement of the oscillator
R_0	Damping coefficient of linear dampers	$\theta_1(t)$	The longitudinal rocking angle displacement of the float at time t
N	Damping coefficient of vertical oscillation	I	The moment of inertia of float around the rotation axis
w	Incident wave frequency	$J_{\Delta\theta}$	Float pitch additional moment of inertia
f	Amplitude of longitudinal rocking excitation moment	θ_2 (t)	The angular shift of the oscillator at time t
k	Spring stiffness	m_{55}	Wave excitation moment generated by the float swing
M	Mass of float	c_{55}	Static water vertical swing recovery torque coefficient

N_θ	The longitudinal damping coefficient		

3. Model construction and solving

3.1. Modeling the motion of floats and oscillators in a wave energy device

In this part, we establish the motion models respectively under two conditions: the damping coefficient of the linear damper is 10000N·s/m and the power of the absolute value of the damping coefficient and the relative velocity of the float and the oscillator is 0.4, and the proportionality coefficient is 10000.

3.1.1. Modeling of oscillators and floats under constant damping

First of all, we have:

$$Q_1 = -R_0\dot{x} + R_0\dot{z}, Q_2 = F_e - F_{Hydrostatic\ Resilience} + R_0\dot{x} - R_0\dot{z} - N\dot{z} \quad (1)$$

According to the kinetic energy theorem:

$$T = \frac{1}{2}(M\dot{z}^2 + m\dot{z}^2) \quad (2)$$

From the elastic potential energy, it can get:

$$V = \frac{1}{2}k(z-x)^2 \quad (3)$$

From the Lagrangian equation, it has:

$$\frac{d}{dt}\left(\frac{\partial T_{KE}}{\partial \dot{z}}\right) - \frac{\partial T_{KE}}{\partial z} + \frac{\partial V}{\partial z} = Q_1 \quad (4)$$

$$\frac{d}{dt}\left(\frac{\partial T_{KE}}{\partial \dot{x}}\right) - \frac{\partial T_{KE}}{\partial x} + \frac{\partial V}{\partial x} = Q_2 \quad (5)$$

The above equations can be solved to derive the differential model of float and oscillator motion, which is shown as follows:

$$(M + M_h)\,\ddot{z} = F_e - (\dot{z} - \dot{x})\,R_0 - N\dot{z} - F_{HR} - k\,(z - x) \quad (6)$$

$$m\ddot{x} = R_0(\dot{z} - \dot{x}) + k\,(z\text{-}x) \quad (7)$$

Since the system is stationary at the initial moment, knowing from the boundary conditions:

When t = 0, $\dot{z} = 0$, z = 0, x = 0, $\dot{x} = 0$, $\dot{z} = \frac{dz}{dt}$, $\dot{x} = \frac{dx}{dt}$, $\ddot{z} = \frac{d\dot{z}}{dt}$ and $\ddot{x} = \frac{d\dot{x}}{dt}$

The damping coefficient of the linear damper in the first case is 10000 N·s/m (i.e., R_0 = 10000, and the period T = 2π/w).

In summary, we build the first motion model:

$$(M + M_h)\,\ddot{z} = F_e - (\dot{z} - \dot{x})\,R_0 - N\dot{z} - F_{HR} - k\,(z - x)$$

$$m\ddot{x} = R_0\,(\dot{z} - \dot{x}) + k\,(z - x)$$

$$F_e = f\cos\,(wt + \varphi)$$

When t = 0, $\dot{z} = 0$, z = 0, x = 0, $\dot{x} = 0$

$$F_{Hydrostatic\ Resilience} = F_{Buoyancy} = \rho\pi r^2 gz$$

$$\dot{z} = \frac{dz}{dt}, \dot{x} = \frac{dx}{dt}, \ddot{z} = \frac{d\dot{z}}{dt}, \ddot{x} = \frac{d\dot{x}}{dt}$$

$$R_0 = 10000$$

3.1.2. Non-constant damping modeling

The damping coefficient of the linear damper is changed, and the change case is to change the damping coefficient from a constant to a first-order differential equation related to the oscillator and float velocities.

And the case of this linear damping coefficient is:

$$R_0 = 10000 * \sqrt{|\dot{z} - \dot{x}|} \quad (8)$$

Where the scale factor is 10000 and the power exponent is 0.5.

In summary, the modified model of the non-constant damping model is as follows:

$$(M + M_h)\,\ddot{z} = F_e - (\dot{z} - \dot{x})\,R_0 - N\dot{z} - F_{HR} - k\,(z - x)$$

$$m\ddot{x} = R_0(\dot{z} - \dot{x}) + k\,(z\text{-}x)$$

$$F_e = f\cos\,(wt + \varphi)$$

$$m\ddot{x} = R_0(-\dot{x}) + k(z-x)$$
$$Q_1 = -R_0\dot{x} + R_0\dot{z}$$
$$Q_2 = F_e + R_0\dot{x} - R_0\dot{z} - N\dot{z}$$
When t = 0, $\dot{z} = 0$, z = 0, x = 0, $\dot{x} = 0$
$$\dot{z} = \frac{dz}{dt},\ \dot{x} = \frac{dx}{dt},\ \ddot{z} = \frac{d\dot{z}}{dt},\ \ddot{x} = \frac{d\dot{x}}{dt}$$
$$R_0 = 10000 * \sqrt{|\dot{z} - \dot{x}|}$$

3.1.3. Model solving

The various parameters at different incident wave frequencies in the model solution are shown in Table 2. The physical and geometric parameter values for the floats and oscillators are shown in Table 3. The relevant data are obtained from the National Marine Science Data Center Network.

Table 2. Various parameters at different incident wave frequencies.

Parameter	Frequency 1	Frequency 2
Incident wave frequency	1.4005 (s^{-1})	2.2143 (s^{-1})
Sag added mass	1335.535 (kg)	1165.992 (kg)
Additional moment of inertia for pitch	6779.315 ($kg \cdot m^2$)	7131.29 ($kg \cdot m^2$)
Damping coefficient of swing wave	656.3616 (N·s/m)	167.8395 (N·s/m)
Damping coefficient of pitch wave	151.4388 (N·m·s)	2992.724 (N·m·s)
Amplitude of heave excitation force	6250 (N)	4890 (N)
Amplitude of pitch excitation moment	1230 (N·m)	2560 (N·m)

Table 3. Physical parameters and geometric parameter values for the floats and oscillators.

Parameter	Short-Cut process	Oscillator height (m)	Short-Cut process
The quality of float	4866 (kg)	Density of sea water	0.5 (kg/m^3)
Bottom radius of float	1 (m)	Density of sea water	1025 (kg/m^3)
Height of cylinder part of float	3 (m)	Spring stiffness	80000 (m)
Height of the cone part of the float	0.8 (m)	Spring the original length	0.5 (m)
Oscillator quality	2433 (kg)	Torsion spring stiffness	250000 (N·m)
Radius of the vibrator	0.5 (m)	Torsion spring stiffness	250000 (N·m)

We use the following steps to complete the model solution process:

1) 0.2s is set as the time step, and the total time is $T_{40-total} = 40 \times 2 \times$ ▯▯▯179.4555s.

2) The second-order binary differential equation is solved by using the fourth-order Runge-Kutta method.

3) The coefficients required for the system of equations are obtained from Table 2 and Table 3. Due to the uncertainty of the phase of the float at the beginning, it is found that it could be taken as φ=0, $F_e = f\cos(wt)$.

4) The displacement and velocity of the obtained float and oscillator are calculated.

5) The above steps are repeated with the float and oscillator motion data recorded every 0.2 seconds during each cycle and graphed from the data.

3.1.4. Model Results

In the case of the fixed damping coefficient and variable damping coefficient, the wave excitation force of float and oscillator is shown in Figure 1.

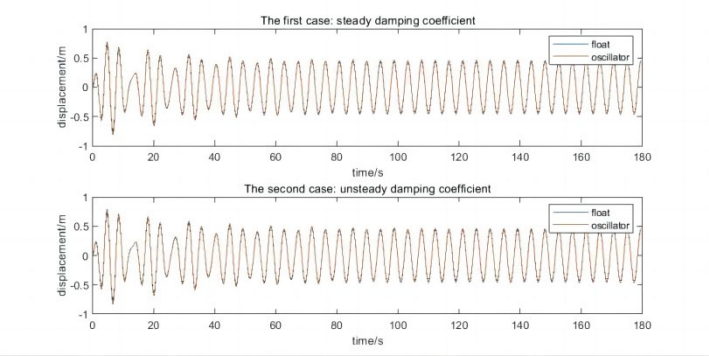

Figure 1. The displacement of the float and the oscillator in both cases

To more clearly explore the vibration law of float and vibrator and judge their vibration types, we compare the relative velocity and relative displacement of float and vibrator under two different damping coefficients. To highlight the contrast effect, the relative displacement and relative velocity of the float relative to the earth and the oscillator relative to the float under different conditions are respectively taken, and the final results are shown in Figure 2 and Figure 3.

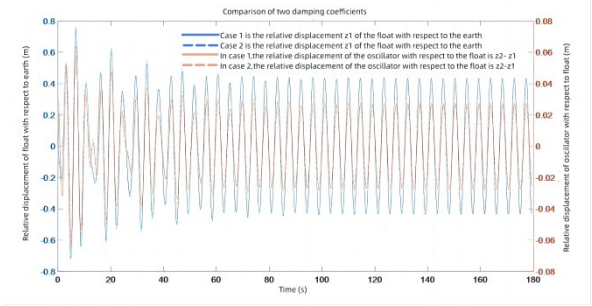

Figure 2. Comparison of z_1,$z_2 - z_1$under different damping conditions

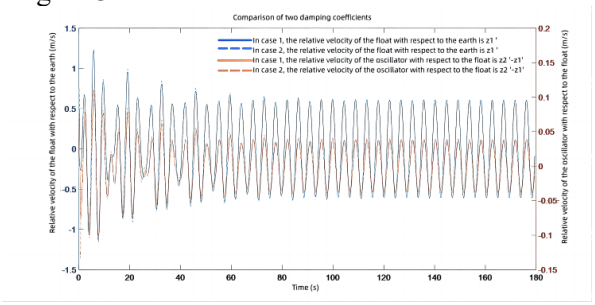

Figure 3. Comparison of $\dot{z}_1$ and $\dot{z}_2 - \dot{z}_1$ under different damping conditions

It can be seen in Figures 1, 2 and 3:

- In both cases, the maximum displacement of the float and oscillator is less than 1m when it is stable.
- When the float and oscillator are just subjected to the wave force, they will do intense movement, and after a period of time, they will do periodic reciprocating motion at the equilibrium position steadily after a period of time.

The above two points show that our model is more reasonable, and is in line with the real situation, the object is disturbed by the first irregular changes and then into a stable simple harmonic movement, which is consistent with our mechanical analysis.

We take the data generated at the time t of 10s, 20s, 40s, 60s, and 100s, and record the data in Tables 4 and 5, respectively.

Table 4. The first case: displacement and velocity of the float and oscillator at a constant damping coefficient.

Time (s)	Float		Oscillator	
	Displacement (m)	Speed (m/s)	Displacement (m)	Speed (m/s)
10	-0.19592	-0.65640	-0.21529	-0.69960
20	0.59255	-0.24046	0.66428	-0.27225
40	0.29545	-0.34343	0.29661	0.33324
60	0.31443	0.49360	-0.35135	-0.51555
100	-0.08359	0.60406	-0.08403	0.623044

Table 5. The second case: displacement and velocity of float and oscillator with unsteady damping coefficient.

Time (s)	Float		Oscillator	
	Displacement (m)	Speed (m/s)	Displacement (m)	Speed (m/s)
10	-0.20547	0.69429	-0.23101	0.69510
20	0.611250	-0.25946	0.68131	-0.20336
40	0.32108	-0.35568	0.29843	0.31039
60	0.31804	0.49596	-0.36836	0.52774
100	-0.08859	0.60406	-0.08403	0.623044

From the model results of the first and the second cases, combined with the data in Table 4 and Table 5, we can see that when the displacement and velocity of the linear damper is constant damping coefficient (i.e., R_0 = 10000) and its damping coefficient is non-constant damping coefficient (i.e., $R_0 = 10000 * \sqrt{|\dot{z} - \dot{x}|}$, the scale factor is 10000, the power is 0.5), the velocity and displacement of the float and the oscillator and the damping coefficient of the damper exist.

3.2. Maximum average power output of the PTO system

In order to increase the application scenario of the mathematical model of the optimal damping coefficient of linear damper, we calculate the maximum output power and corresponding optimal damping coefficient of the following two cases respectively:

- The damping coefficient is constant and takes a value within the interval [0, 100000].
- The damping coefficient is proportional to the power exponent of the absolute value of the relative velocities of the float and vibrator. The scale coefficient is valued in the interval [0, 100000], and the power exponent is valued in the interval [0, 1].

3.2.1. Constant damping coefficient modeling

A mathematical planning optimization model is established with the following variables and constraints:

1) Objective function: the average output power of the damper.

The study shows that the total power of the PTO system is equal to the sum of the spring power and the damper power, but because the elastic potential energy generated by the PTO system cannot be transferred directly to the generator, the average output power of the PTO system cannot be calculated directly. We can solve this by calculating the total average power of the spring and damper over 40 cycles.

The average output power of the spring is:

$$\overline{P} = \frac{1}{T}\int_0^T R_0\,(\dot{z} - \dot{x})^2 \tag{9}$$

$$Z = \max\,(\overline{P}) \tag{10}$$

2) Decision-making variables:

$$R_0 \in [0, 100000] \tag{11}$$

3) Constraints:

Hydrodynamic equation constraint:

$$\left(M_f + M_h\right)\ddot{z} + R_{pto}(\dot{z} - \dot{x}) + N\dot{z} + Kz + k\,(z - x) = F_e \tag{12}$$

$$m\ddot{x} = R_0\,(\dot{z} - \dot{x}) + k - (z - x) \tag{13}$$

Under periodic constraints, to determine a more stable maximum average output power, we will select at least 40 cycles to solve the maximum average output power, namely: $\mathbf{T \geq 40\frac{2\pi}{w}}$.

The overall mathematical planning optimization model is as follows:

$$\overline{P} = \frac{1}{T}\int_0^T R_0\,(\dot{z} - \dot{x})^2$$

$$Z = \max\,(\overline{P})$$

$$(M_f + M_h)\ddot{z} + R_{\mathrm{PTO}}(\dot{z} - \dot{x}) + N\dot{z} + F_{HR} + k(z - x) = F_e$$

$$\mathrm{m}\ddot{\mathbf{x}} = \mathbf{R_0}(\dot{\mathbf{z}} - \dot{\mathbf{x}}) + \mathrm{k}\ (\mathrm{z\text{-}x})$$

$$\mathrm{T} \geq \mathbf{40}\frac{\mathbf{2\pi}}{\mathbf{w}}$$

3.2.2. Modeling of unsteady damping coefficient

As the modeling process is similar to the above, only the damping coefficient becomes $R_0 = 100000 * \sqrt{|\dot{z} - \dot{x}|}$. Therefore, we omit the modeling process, and the following is the new mathematical model:

$$\overline{P} = \frac{1}{T}\int_0^T R_0(\dot{z} - \dot{x})^2$$

$$Z = max\ (\overline{P})$$

$$\left(M_f + M_h\right)\ddot{z} + R_{pto}(\dot{z} - \dot{x}) + N\dot{z} + Kz + k\ (z - x) = F_e$$

$$m\ddot{x} = R_0(\dot{z} - \dot{x}) + k\ (z\text{-}x)$$

$$T = \frac{1}{2}(M\dot{z}^2 + m\dot{z}^2)$$

$$V = \frac{1}{2}k(z - x)^2$$

3.2.3. Constant damping factor model solving

If only the traversal method is used to solve the average output power of the PTO system, the time complexity is relatively high and the comparison experiment is lacking. In order to calculate the average power of the spring and the average power of the damper more accurately and quickly, we use the traversal method and the genetic algorithm to solve the model respectively. Because the traversal algorithm idea is relatively simple, we omit the list.

The wave energy coefficient identified by the genetic algorithm means that the wave energy calculation model is embedded in the genetic algorithm in the mathematical model [6], and the process is shown in Figure 4.

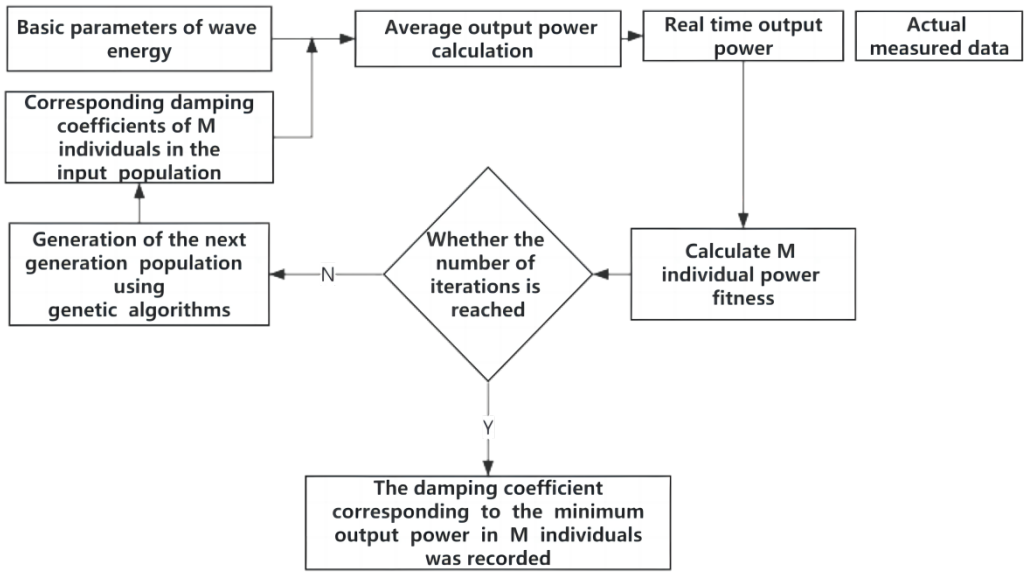

Figure 4. Genetic algorithm solving flow chart

The specific implementation steps of the genetic algorithm are as follows:

1) The basic parameters of wave energy and the number of iterations are set.

2) The number of individuals in the population is denoted as M, and the corresponding damping coefficient of M individuals is in the input population.

3) The objective function is defined and the corresponding average output power $\overline{P}$ is calculated.

4) The real-time output power $P(t)$ at fixed intervals (0.1s here) is calculated and recorded.

5) The phase adjustment of M individuals is calculated by comparing the actual measured data with the real-time output power.

6) Whether the set number of iterations is reached is checked. If it is not reached, the genetic algorithm is used to generate a new generation of population and return to step 2. If it is reached, the damping coefficient corresponding to the minimum output power in M individuals is recorded, and the cycle ends.

3.2.4. Model Results

3.2.4.1 Constant damping coefficient

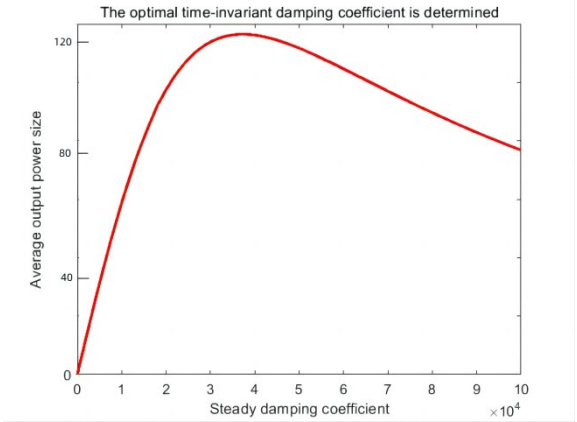

Figure 5. The graph of the optimal constant damping coefficient is solved by the traversal method

As can be seen from Figure 5, the curves of the maximum average output power and optimal constant damping coefficient solved by the traversal method show a trend of first increasing and then decreasing, indicating that the model conforms to the normal actual situation. It can be concluded from the figure that the optimal average output power is 121.18 W and the optimal constant damping coefficient is 3.27×10^4N·s/m.

3.2.4.2 Unsteady damping coefficient

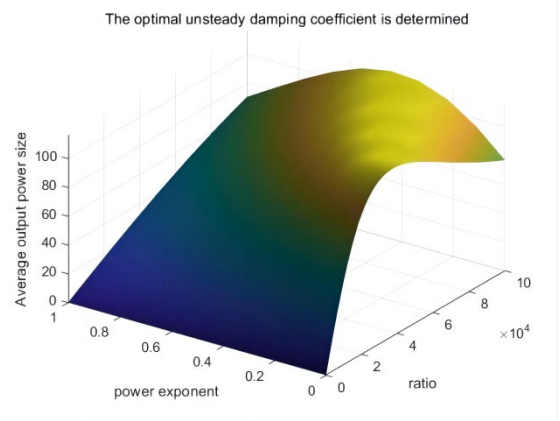

Figure 6. Iteration to find the optimal non-constant damping factor graph

From Figure 6, it can be concluded that when the traversal method is used to solve the unsteady damping coefficient, the proportional coefficient and power index corresponding to the maximum average output power of the PTO system are obtained, thus determining the optimal unsteady damping coefficient. As

can be seen from the figure, the 3D model is a surface that gradually increases and then decreases from both sides, which conforms to the model law of this problem. It can be obtained from the figure that the optimal average output power is 121.1008 W and the optimal steady-state damping coefficient is 3.27×10^4 N·s/m.

In order to ensure the accuracy of the experimental results, we use the genetic algorithm to solve the optimal abnormal damping coefficient of this problem again for the comparison experiment. The specific algorithm idea and process are shown in Figure 4. The final result is Figure 7.

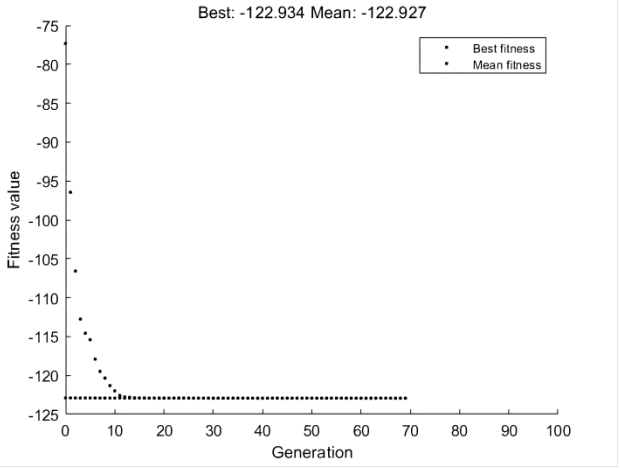

Figure 7. Genetic algorithm is used to solve the optimal non-constant damping coefficient

As can be seen from Figure 7, we have basically reached the maximum output power in the 12th iteration by using the genetic algorithm, and the output power is basically unchanged in the subsequent iterations. So we get Max ($\overline{P}$) = 122.934 W. The results are similar to those obtained by the traversal method, which shows that the calculated results have a certain precision.

3.2.5. Time contrast

Table 6. Comparison of time used by different algorithms.

The traversal algorithm	991.177 (s)
Genetic algorithm	118.231 (s)

From Table 6, we see that when solving the optimal unsteady damping coefficient, the time spent by using the traversal method is 838.34% of the time spent by using the genetic algorithm. Therefore, genetic algorithms have a faster processing speed when solving similar problems compared to the traversal method.

4. Conclusion

In this paper, we solve the motion model of float and oscillator by Lagrangian equation, which makes our model the solid and reliable physical principle and mathematical foundation, and its theoretical part is highly convincing, credible and easier to be understood and learned. The optimization model of the output power is solved by using the genetic algorithm, which makes our model results clearer and the calculation process more transparent, and it also compares the genetic algorithm with the traversal method, which can help you choose the algorithm better when studying this problem. The model in this paper does not take into account the effect of friction and should be derived by the energy method. The model has high availability and can be extended to different locations in the water with waves to study and explore the energy problem in the wave vibration problem. We can extend the corresponding model to the air, for example, to explore the movement of hot air balloons through the air. At the same time, you can also focus on the energy side and compare the seismic waves. At the same time, the model is also suitable for the viscous fluid swamp, debris flow [7], etc. Therefore, the model also has a wide

application prospect in the prevention of natural disasters. Finally, it also provides a reference for exploring the maximization of the energy utilization model [8].

References

[1] Caiyun Gao. Several algorithms for the rotational inertia of homogeneous rigid bodies [J]. Journal of Shanxi Datong University (Natural Science Edition), 2022, 38 (04): 17 - 21.
[2] Zhang Baocheng, Deng Ziwei, Miao Yu, et al. Study on the factors influencing the hydrodynamics of point absorption oscillating float [J]. Journal of Solar Energy, 2022, 43 (04): 512 - 518.
[3] Ao Jingtao. Study on hydrodynamic and energy conversion characteristics of moon pool floating wave energy device [D]. Harbin Engineering University, 2020.
[4] Zhou YY, Li BQ, Cai Zongju, et al. Float motion and load analysis of gyroscopic wave energy generation device [J]. Ship and Sea Engineering, 2016, 45 (03): 90 - 98.
[5] Hu Qingsong, Zheng Bo, Cao Jiarui, Chen Leilei, Li Jun, RAHMAN Hafiz Abdur. Design and experiment of balanced buffeting system of shipborne bait casting device [J]. Journal of Shanghai Ocean University, 2020, 29 (06): 928 - 937.
[6] Zhong Yao, Sun Li, Liu Gongpeng. General layout design of an offshore test site for wave and tidal energy [J]. Hydropower, 2013, 39 (11): 91 - 93.
[7] Gui-ling Wang, Wei Zhang, Feng Ma, Wen-jing Lin, Ji-yun Liang, Xi Zhu. Overview of hydrothermal and hot dry rock research in China [J]. China Geology, 2018, 1 (02): 273 - 285.
[8] Chen Xilong, Wang Zhiping, Gu Hanbin, Xiong Wei, Pan Guifeng. Zhoushan sea wave energy plan and outlook of development and utilization mode [J]. Journal of Zhejiang electric power, 2018, 5 (6): 30 - 35, DOI: 10.19585 / j.z JDL. 201806007.